33 Stämpfli, R., and Hille, B., Electrophysiology of the peripheral myelinated nerve; in: Frog neurobiology, pp. 3–32. Eds R. Llinas and W. Precht. Springer, Berlin/Heidelberg/New York 1976.
34 Tao-Cheng, J.-H., and Rosenbluth, J., Nodal and paranodal membrane sturcture in complementary freeze-fracture replicas of amphibian peripheral nerves. Brain Res. *199* (1980) 249–265.
35 Vallbo, Å.B., Accomodation related to inactivation of the sodium permeability in single myelinated nerve fibers from *Xenopus laevis*. Acta physiol. scand. *61* (1964) 429–444.
36 Waxman, S.G., and Foster, R.E., Ionic channel distribution and heterogeneity of the axon membrane in myelinated fibers. Brain Res. Rev. *2* (1980) 205–234.
37 Wiley, C.A., and Ellisman, M.H., Rows of dimeric-particles within the axolemma and juxtaposed particles within glia, incorporated into a new model for the paranodal glial-axonal junction at the node of Ranvier. J. Cell Biol. *84* (1980) 261–280.

0014-4754/83/090964-13$1.50+0.20/0

VII. The myelinated nerve: Some unsolved problems

by B. Neumcke

I. Physiologisches Institut, Universität des Saarlandes, D-6650 Homburg/Saar (Federal Republic of Germany)

The previous chapters of this multi-author review have illustrated that the electrophysiological and morphological properties of myelinated nerve fibers are intimately related. For example, the kinetics of drug action described in the chapter by Ulbricht cannot be interpreted without a detailed knowledge of the nodal architecture (see the contribution by Berthold and Rydmark), and the identification of intramembranous nodal particles with ionic channels as suggested by Rosenbluth would be very vague without the determination of channel numbers from electrophysiological measurements (compare the section by Schwarz). In the following we want to list some properties of myelinated nerve fibers which are not yet fully understood and which may be elucidated by future electrophysiological and morphological investigations.

Myelinated nerve fibers may be classified according to their function (motor or sensory fiber) or according to their origin (amphibian or mammalian fiber). All different types of fibers exhibit different conduction properties. These electrophysiological differences are not only apparent in the various shapes of the action potentials but are already expressed by different ionic permeabilities in the resting state. Thus the resting potassium conductance of a frog motor fiber is larger than the one of a sensory fiber while the magnitude of the resting potential is comparable in both cases[10].

Significant differences in the generation of resting potentials also seem to exist between amphibian and mammalian myelinated nerve fibers: For frog nerve fibers the resting potential in Ringer's solution containing 2.5 mM K^+ ions is −71 mV at 17 °C as measured with a 'cover-slip' method[5]. Figure 1 shows the determination of the resting potential of a single rat myelinated nerve fiber by a similar technique (for details see the legend). At a temperature of 21 °C the resting potential of the fiber was only −50 mV and no action potentials could be elicited from this level not even by strong depolarizing current pulses. Hence the resting potential in vivo must be more negative and it is then probably not controlled entirely by passive ionic membrane permeabilities. The temperature dependence of the resting potential of the isolated rat nerve fiber (fig. 1) also suggests that active metabolic processes may be decisive in the function of mammalian myelinated nerve fibers. On the other hand, no such pronounced effect of temperature on the resting potential of isolated frog myelinated nerve fibers could be observed (B. Neumcke and R. Stämpfli, unpublished).

The most striking difference between amphibian and mammalian nerve fibers is the virtual absence of

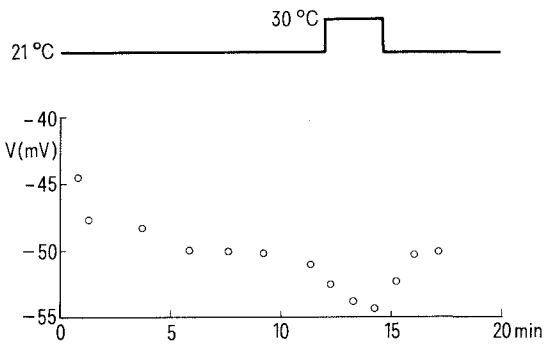

Figure 1. Resting potential V of a single myelinated fiber from a rat sciatic nerve. A 4–5 mm section of the fiber with adherent nerve trunks on both sides was mounted in the recording chamber in which all compartments were flooded with extracellular solution. The fluid level was then lowered until the compartments were separated from each other. The compartment containing the test node (A pool) remained filled with flowing extracellular solution whereas the solution in the neighboring pools was replaced by isotonic KCl. In one of these side compartments (C pool) the fiber was cut beyond the neighboring node. The resting potential V of the test node was then determined as the voltage from an external source between pools A and C at which no injury current between A and C could be detected. Symbols represent measurements of V at various times after cutting the fiber in the C pool. Note the reversible decrease of V after a temperature increase of the extracellular solution from 21 to 30 °C. The extracellular solution contained 154 mM NaCl, 2.2 mM $CaCl_2$, 5.6 mM KCl and 10 mM morpholinopropanesulphonic acid at pH 7.2. Isotonic KCl solution was composed of 155 mM KCl, 5 mM NaCl and 10 mM morpholinopropanesulphonic acid at pH 7.2. Experiment 42/82 (Neumcke and Stämpfli, unpublished).

potassium currents in intact mammalian nodes (compare the preceding chapters by Stämpfli, Schwarz and Brismar). The repolarization of the action potential down to the resting level has then to be accomplished by outward leakage currents alone[2], and differences in the repolarization phases of motor and sensory action potentials can no longer be attributed to different potassium conductances in both types of fibers. It is not yet clear which ionic processes cause the different shapes of action potentials in motor and sensory mammalian nerve fibers. It has been speculated that the leakage conductance may be distinct in both types of fibers[6]. Another candidate for the difference is the sodium conduction system, in particular the process of sodium inactivation. As shown first for frog nerve fibers the kinetics of sodium inactivation are non-exponential but may be satisfactorily described as sum of two exponential functions[1]. A difference in the ratio of the amplitudes of the fast and slow inactivation phases can contribute to the observed shorter duration of the sensory action potential of a frog nerve fiber[8]; perhaps it also could explain the distinct repolarization phases of motor and sensory action potentials in mammalian nodes.

The nonexponential kinetics of sodium current inactivation are a characteristic feature of myelinated nerve, in all other excitable tissues (e.g. in the squid giant axon) the deviation of the decline of sodium currents from an exponential function is much less pronounced. The behavior has been taken as evidence that the process of sodium inactivation in myelinated nerve is governed by a process of second order[1]. It is, however, difficult to understand that the gating of sodium channels in myelinated nerve should be distinct from that of sodium channels in other excitable membranes. Also, the kinetics of sodium current inactivation in myelinated nerve are not strictly biexponential: The fit of the declining phase of the sodium currents by the sum of two exponential functions often yields different fit curves of the same quality depending on the choice of the initial fit parameters (B. Neumcke and W. Schwarz, unpublished). Instead of proposing that sodium inactivation is a process of third or even higher order, it seems to be more realistic to discuss other alternatives which could account for the peculiar sodium current inactivation in myelinated nerve. A possible origin of this behavior is the restricted access of Na^+ ions to the nodal membrane through the nodal gap as well as the reduced cation diffusion coefficient and the small diffusion space in the axoplasm. Such diffusion limitations could be responsible for the deviations of sodium current inactivation from an exponential function in myelinated nerve. A consequence of this hypothesis would be that such diffusion limitations should be different in motor and sensory nerve fibers to account for alterations of sodium current inactivation between the two types of nerve fibers[8]. This could be tested by comparing the transients of sodium currents after a sudden solution exchange (compare the chapter by Ulbricht) or the morphology of the nodal gap (see the section by Berthold and Rydmark) in motor and sensory nerve fibers.

Until recently it was thought that the nodal membrane of myelinated nerve would contain only 2 types of ion-selective channels being uniformly distributed over the membrane surface: Sodium channels and delayed rectifier potassium channels. Since the discovery of the absence of potassium currents in intact mammalian nodes and their appearance after enzyme treatment or application of hypertonic solution, the opinion now is that sodium channels are concentrated in the middle portion of the nodal membrane whereas potassium channels are located more towards the paranodal regions. This segregation of sodium and potassium channels gives further evidence for the view that both types of channels are separate entities of the nodal membrane and that their gating processes are not linked with each other. It is not yet known whether a similar segregation prevails in the nodal membrane of amphibian nerve fibers. Experiments with specific markers for sodium and potassium channels or the comparison of sodium and potassium current transients after an exchange of the extracellular solution could help to answer this question. Not only the arrangement of sodium and potassium channels has been reviewed recently but also the concept of only two types of ionic channels in the nodal membrane: it now appears that there are different potassium channels in the nodes of frog nerve which exhibit different gating kinetics, are selectively blocked by various substances and are present in different portions in motor and sensory nerve fibers[4]. The physiological significance of the various potassium channels is still obscure, nor is it known whether all types of potassium channels are located in the same areas of the nodal membrane, and whether they are also present in exposed mammalian nodes or in pathological nerve fibers.

The electrical properties of single ionic channels in excitable membranes are best studied with the so called 'patch-clamp' technique in which one or a few channels are electrically isolated from the rest of the channels by pressing a micropipette against the membrane. Due to the small width of the nodes of Ranvier and the presence of microvilli of Schwann cells in the nodal gap (see the contribution by Berthold and Rydmark) this technique may not be applicable to myelinated nerve fibers. Hence the properties of nodal ionic channels must still be extracted from the ionic and gating currents measured from all channels in one node (compare the chapter by Schwarz). Nevertheless, this approach may contribute to the understanding of the gating of single channels, to the

mechanism of the creation of new and the decay of existing channels, and to the detection of interactions among neighboring channels:

Figure 2 illustrates an experiment from which the probability p of the open state of sodium channels can be derived at various times after a depolarizing voltage step. Part A shows the kinetics of the sodium current, I, with the familiar fast current activation up to a peak value followed by a slower inactivation phase. The variance, var, of sodium-current fluctuations in the same time range, as measured by an ensemble average method[9], is illustrated in part B. The points in part C are obtained by plotting isochronical (var, I) pairs from parts A and B. A parabola has been fitted to the points, and the current i through one open sodium channel and the number N of channels per node may be calculated from the fitted parameters (for details see the legend to the figure). The probability p(t) of the open-channel state is then given by $p(t)=I(t)/(Ni)$ and thus can be obtained at various times t after the onset of the depolarization. Its maximum value of 0.77 is reached at the time of the peak sodium inward current. As explained in the legend to figure 2 such high values of p cannot be obtained from gating mechanisms in which the processes of sodium activation and inactivation proceed independently of each other (e.g. from the Hodgkin-Huxley m^3 h formulation). That sodium activation and inactivation are at least partially coupled with each other follows also from an analysis of stationary current fluctuations[3]. This demonstrates how current measurements on a large number of ionic channels can limit the range of acceptable models for gating of an individual channel.

The number of functioning channels in a biological membrane is not a fixed quantity and can be modified by various means. An impressive example is the creation (or decay) of activatable sodium channels in the nodal membrane after holding the fiber at more negative (positive) membrane potentials[7]. Similar to the generation of gramicidin and alamethicin pores in lipid bilayer membranes by electric fields the increase of the number of sodium channels with hyperpolarization could be a field-induced aggregation of already existing precursors to a new ionic channel. However, it is difficult to understand that such an aggregation requires several min in the nodal membrane while the formation of pores in lipid bilayers takes place in the msec time range. It would be of great interest to investigate whether the alteration of the number of activatable sodium channels would be correlated with a similar change of the density of intramembranous particles. Such combined electrophysiological and morphological studies could corroborate the identification of particles with channels and would help to clarify the dynamics of membrane channels.

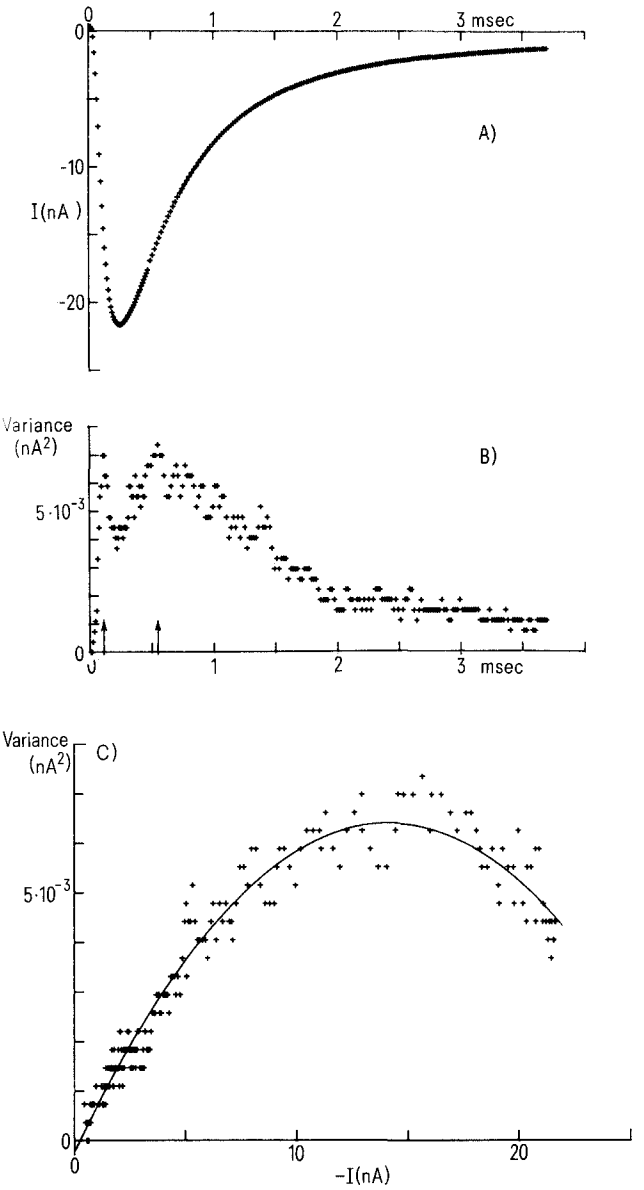

Figure 2. Sodium currents and sodium-current fluctuation in a frog myelinated nerve fiber.
A Kinetics of sodium current, I, after a depolarization to −10 mV from a holding potential of −98 mV. The extracellular solution contained 110.5 mM NaCl, 2 mM $CaCl_2$, 10 mM tetraethylammonium chloride, 4 mM morpholinopropanesulphonic acid at pH 7.2 and 8 nM tetrodotoxin. The ends of the fiber were cut in a solution containing 113 mM CsCl and 7 mM NaCl. The peak of the sodium inward current $I^{peak}=-21.7$ nA is reached at $t^{peak}=0.25$ msec, the early phase of sodium inactivation follows the curve $A\cdot\exp(-t/\tau)$ with A = −34 nA and $\tau=0.69$ msec. The probability p of the open-channel state at $t=t^{peak}$ must be smaller than $\exp(-t^{peak}/\tau)=0.70$ if the processes of sodium activation and inactivation would be independent of each other.
B Ensemble average values of the variance, var, of sodium-current fluctuations. Arrows indicate the locations of the variance maxima. Since var is proportional to p(1-p), it is p = 0.5 at the maxima and p > 0.5 between the maxima.
C Var as function of I. From the parabola $var=iI-I^2/N+c$ fitted to the points one obtains the current i = −0.942 pA through one open sodium channel, the number $N=29.9\cdot10^3$ of sodium channels per node and the variance $c=-2.26\cdot10^{-4}$ nA^2 of contributions not arising from sodium channels[9]. The probability at the peak sodium current is $p^{peak}=I^{peak}/(Ni)=0.77$. Experiment 23/82, motor fiber, temperature 15 °C (Neumcke and Stämpfli, unpublished).

The nodal membrane of amphibian and mammalian myelinated nerve fibers contains sodium channels with a high surface density of 1000–2000/μm^2. The corresponding average distance 20–30 nm between channels is so small that interactions between neighboring channels could occur. Indeed, the conductance of a single sodium channel in a frog nerve fiber is higher when the number of activatable channels is reduced either by a more positive holding potential or by the addition of the sodium-channel blocker tetrodotoxin[7]. This seems to indicate that the ion flux through one open channel is hindered by the ion flux through neighboring channels. The nodal membrane is an ideal preparation to study such channel-channel interactions because of the extremely high channel density. Yet the total channel number per node is still low enough to allow the simultaneous measurement of sodium currents and sodium-current fluctuations with conventional analog-to-digital converters. Interactions between neighboring ionic channels could affect not only their conductances but also the gating kinetics of individual channels. It would be of great interest to investigate whether peculiarities of the kinetics of ionic currents in myelinated nerve (e.g. the pronounced non-exponential sodium inactivation) could originate in such interactions. It also seems to be promising to study possible channel-channel interactions in other membranes with a lower overall channel surface density. Significant interactions would then indicate that the channels are not equally distributed over the membrane but are probably arranged within local clusters of more channels.

The above list of still unexplained properties of myelinated nerve fibers is by no means complete, and the selection of the topics has been biassed by the author's own electrophysiological investigations. It is hoped, however, that the examples mentioned in this chapter and the contents of all previous sections of this multi-author review have illustrated the close interrelations between the electrical and structural aspects of myelinated nerve fibers and the importance of future electrophysiological and morphological investigations which may contribute to a better understanding of the function of myelinated nerve fibers.

1 Chiu, S.Y., Inactivation of sodium channels: Second order kinetics in myelinated nerve. J. Physiol. *273* (1977) 573–596.
2 Chiu, S.Y., Ritchie, J.M., Rogart, R.B., and Stagg, D., A quantitative description of membrane currents in rabbit myelinated nerve. J. Physiol. *292* (1979) 149–166.
3 Conti, F., Neumcke, B., Nonner, W., and Stämpfli, R., Conductance fluctuations from the inactivation process of sodium channels in myelinated nerve fibres. J. Physiol. *308* (1980) 217–239.
4 Dubois, J.M., Evidence for the existence of three types of potassium channels in the frog Ranvier node membrane. J. Physiol. *318* (1981) 297–316.
5 Huxley, A.F., and Stämpfli, R., Direct determination of membrane resting potential and action potential in single myelinated nerve fibres. J. Physiol. *112* (1951) 476–495.
6 Neumcke, B., and Stämpfli, R., Sodium currents and sodium-current fluctuations in rat myelinated nerve fibres. J. Physiol. *329* (1982) 163–184.
7 Neumcke, B., and Stämpfli, R., Alteration of the conductance of Na^+ channels in the nodal membrane of frog nerve by holding potential and tetrodotoxin. Biochim. biophys. Acta *727* (1983) 177–184.
8 Schwarz, J.R., Bromm, B., and Ochs, G., Inactivation of sodium permeability in motor and sensory nerve fibres. Pflügers Arch. *389* (1981) R 23.
9 Sigworth, F.J., The variance of sodium current fluctuations at the node of Ranvier. J. Physiol. *307* (1980) 97–129.
10 Stämpfli, R., Is the resting potential of Ranvier nodes a potassium potential? Ann. N.Y. Acad. Sci. *81* (1959) 265–284.

0014-4754/83/090976-04$1.50 + 0.20/0

Full Papers

The effect of digitoxose on feeding behavior

D.F. Brown[1] and J.M. Viles[2]

Molecular, Cellular, Developmental Biology Program, and Department of Zoology, Iowa State University, Ames (Iowa 50011, USA), January 12, 1983

Summary. The effect of digitoxose (DIG) on food intake, gold thioglucose (GTG) lesion formation in the ventromedial hypothalamus (VMH), and VMH glucose oxidation in vitro was investigated in mice. DIG significantly decreased the amount of food ingested during the day compared to controls ($p < 0.01$). DIG had no effect on nocturnal feeding. GTG lesion formation in the VMH and VMH glucose oxidation were not altered by DIG treatment. These results suggest that DIG alters daytime feeding behavior by affecting extrahypothalamic or peripheral glucoreceptor sites.